

Observation of strongly forbidden solid effect dynamic nuclear polarization transitions via electron-electron double resonance detected NMR

Cite as: J. Chem. Phys. **139**, 214201 (2013); <https://doi.org/10.1063/1.4832323>

Submitted: 06 September 2013 . Accepted: 06 November 2013 . Published Online: 04 December 2013

Albert A. Smith, Björn Corzilius, Olesya Haze, Timothy M. Swager, and Robert G. Griffin



View Online



Export Citation



CrossMark

ARTICLES YOU MAY BE INTERESTED IN

Overhauser effects in insulating solids

The Journal of Chemical Physics **141**, 064202 (2014); <https://doi.org/10.1063/1.4891866>

Solid effect in magic angle spinning dynamic nuclear polarization

The Journal of Chemical Physics **137**, 054201 (2012); <https://doi.org/10.1063/1.4738761>

Solid effect dynamic nuclear polarization and polarization pathways

The Journal of Chemical Physics **136**, 015101 (2012); <https://doi.org/10.1063/1.3670019>

Lock-in Amplifiers

Zurich Instruments

Watch the Video

Observation of strongly forbidden solid effect dynamic nuclear polarization transitions via electron-electron double resonance detected NMR

Albert A. Smith,^{a)} Björn Corzilius,^{b)} Olesya Haze, Timothy M. Swager,
and Robert G. Griffin^{c)}

Department of Chemistry and Francis Bitter Magnet Laboratory, Massachusetts Institute of Technology,
Cambridge, Massachusetts 02139, USA

(Received 6 September 2013; accepted 6 November 2013; published online 4 December 2013)

We present electron paramagnetic resonance experiments for which solid effect dynamic nuclear polarization transitions were observed indirectly via polarization loss on the electron. This use of indirect observation allows characterization of the dynamic nuclear polarization (DNP) process close to the electron. Frequency profiles of the electron-detected solid effect obtained using trityl radical showed intense saturation of the electron at the usual solid effect condition, which involves a single electron and nucleus. However, higher order solid effect transitions involving two, three, or four nuclei were also observed with surprising intensity, although these transitions did not lead to bulk nuclear polarization—suggesting that higher order transitions are important primarily in the transfer of polarization to nuclei nearby the electron. Similar results were obtained for the SA-BDPA radical where strong electron-nuclear couplings produced splittings in the spectrum of the indirectly observed solid effect conditions. Observation of high order solid effect transitions supports recent studies of the solid effect, and suggests that a multi-spin solid effect mechanism may play a major role in polarization transfer via DNP. © 2013 AIP Publishing LLC. [<http://dx.doi.org/10.1063/1.4832323>]

I. INTRODUCTION

Dynamic nuclear polarization (DNP) is a method of signal enhancement in nuclear magnetic resonance (NMR) experiments which involves the transfer of the large electron polarization to the nuclear spin system.^{1,2} In recent years, the state of the art of DNP experiments has improved dramatically with the introduction of many new radicals^{3–11} and improved technique and instrumentation.^{12–16} Because NMR is an inherently insensitive technique, DNP allows prohibitively long experiments to become feasible. There are a variety of recent applications of DNP including biological studies,^{17–22} surface studies,²³ and dynamics studies^{24,25} which would not otherwise be possible.

Aside from pulsed-DNP, microwave-driven DNP mechanisms in the solid-state can be categorized into three mechanisms, depending on the relative sizes of the homogenous linewidth (δ), the inhomogeneous linewidth (Δ), and the nuclear Larmor frequency (ω_{0I}): The solid effect (SE) is a two-spin mechanism where microwave irradiation simultaneously flips an electron and nucleus, and is dominant when $\omega_{0I} > \delta, \Delta$.^{26,27} The cross effect (CE) is a three-spin mechanism, for which microwave irradiation saturates one electron, and then a three-spin electron-electron-nuclear transition polarizes the nucleus. CE is dominant when $\delta < \omega_{0I}$

$< \Delta$.^{28–30} Thermal mixing is a multi-electron process similar to CE which results in a nuclear spin flip and is dominant when $\omega_{0I} < \delta, \Delta$.^{31–33}

Continued advancement of DNP requires a better understanding of the transfer mechanisms, and recently there has been a renewed effort to better characterize the SE. In the case of an electron-nuclear pair, it is straightforward to obtain the transition probability and matching condition of the SE. The latter is given by $\Delta\omega_{0S} = \pm\omega_{0I}$, where $\Delta\omega_{0S}$ is the offset of the microwave frequency from the electron Larmor frequency.^{34,35} However, the multiple-spin mechanism is far more complicated, because of higher order spin interactions that are accessible in strongly coupled systems, and because of the role that spin-diffusion plays in transporting polarization from an electron to the bulk nuclei that are observed in NMR. Hovav *et al.* described a variety of simulations of the SE that highlight the complicated nature of the matching condition.³⁶ They also discuss the role that higher order interactions play in the polarization of bulk nuclei for larger spin systems.³⁷ We have also been working to elucidate details of the SE mechanism for multiple spins via experimental methods. Recent experiments were performed on static samples for which nuclear polarization buildup rates and enhancements were measured. We explained our results with a model in which nuclei near an electron compete with bulk nuclei for polarization, and therefore deplete the final bulk polarization.³⁸ More recently, we showed that our model is consistent with results obtained for samples in magic angle spinning (MAS) experiments.³⁹

In this paper, we focus on the SE DNP mechanism, which we observe indirectly via loss of electron polarization. The advantage of this indirect observation is that it provides

^{a)}Current address: Department of Chemistry and Applied Biosciences, Laboratory of Physical Chemistry, ETH-Zürich, CH-8093 Zürich, Switzerland.

^{b)}Current address: Institute for Physical and Theoretical Chemistry, Institute for Biophysical Chemistry, and Center for Biomolecular Magnetic Resonance (BMRZ), Goethe University, Max-von-Laue-Str. 7-9, 60438 Frankfurt am Main, Germany.

^{c)}Author to whom correspondence should be addressed. Electronic mail: rgg@mit.edu

insight into the DNP processes occurring near the electron, rather than only seeing the results of DNP on the bulk nuclear polarization. Our experiments utilize trityl radical and a water-soluble BDPA (SA-BDPA),⁷ and are performed at 5 T (140 GHz EPR, 211 MHz ¹H frequency).⁴⁰ We irradiate the sample with a swept microwave frequency, followed by detection of the electron polarization via a Hahn echo. Schosler *et al.* originally introduced a very similar sequence, in order to record broad hyperfine lines, free of distortion,⁴¹ and the approach has recently seen application in studies of water binding in Photosystem II,⁴⁴ being a useful alternative to ENDOR experiments.^{42,43} In our case, however, we use the sequence to characterize the SE DNP mechanism. In our experiments, rather than only observing a decrease in the electron polarization at the SE matching condition, as one might expect from basic SE theory and other recent results,⁴⁵ we observe polarization depletion at the SE matching condition and additionally at $\Delta\omega_{0S} = \pm n\omega_{0I}$, where $n = 2, 3, 4$, which correspond to higher-order SE conditions. These results are compared to the enhancement of bulk nuclear polarization, observed via NMR, where enhancement is only seen for $n = 1$. We also see that the SE matching condition is split into many peaks by hyperfine coupling to nearby protons when using SA-BDPA, which has many protons strongly coupled to the electron.

II. THEORY

In order to gain insight into the SE mechanism, we start by considering the Hamiltonian of a system of many nuclei in the rotating frame of the microwave field,

$$\begin{aligned} H &= H_Z + H_{IS} + H_{II} + H_M \\ H_Z &= \Delta\omega_{0S}S_z - \sum_j \omega_{0I,j}I_{jz} \\ H_{IS} &= \sum_j (A_j S_z I_{jz} + B_j S_x I_{jx} + C_j S_y I_{jy}) \quad (1) \\ H_{II} &= \sum_j \sum_{k>j} \vec{I}_j \vec{\vec{D}}_{j,k} \vec{I}_k \\ H_M &= \omega_{1S}S_x. \end{aligned}$$

H_Z contains the Zeeman interactions where $\Delta\omega_{0S}$ is the microwave frequency offset and the $\omega_{0I,j}$ are the nuclear Zeeman frequencies. H_{IS} is the electron-nuclear coupling where A_j , B_j , and C_j are the couplings in the z , x , and y directions. H_{II} is the nuclear-nuclear coupling where $\vec{\vec{D}}_{j,k}$ is the nuclear-nuclear coupling tensor. Finally, H_M is the microwave field where ω_{1S} is its field strength. It is straightforward to diagonalize $H_Z + H_{IS}$, by first rotating each nucleus about the z -axis by an angle χ_j using the unitary operator U_χ (H_Z is invariant to this rotation so we only show H_{IS}), which leads to

$$\begin{aligned} U_\chi &= \prod_j \exp[i\chi_j I_{jz}] \\ \tan \chi_j &= C_j/B_j \quad (2) \\ U_\chi H_{IS} U_\chi^{-1} &= \sum_j (A_j S_z I_{jz} + (B_j^2 + C_j^2)^{1/2} S_x I_{jx}). \end{aligned}$$

We define $B_j^* = (B_j^2 + C_j^2)^{1/2}$ for convenience, and complete the diagonalization of $H_Z + H_{IS}$ by repeating the steps given by Hu *et al.*³⁵ for each nucleus, resulting in

$$\begin{aligned} U_\eta &= \prod_j \exp[i(\eta_{\alpha,j} - \eta_{\beta,j})S_z I_{jy} \\ &\quad + \frac{i}{2}(\eta_{\alpha,j} + \eta_{\beta,j})I_{jy}] \\ \tan \eta_{\alpha,j} &= \frac{B_j^*}{A_j - 2\omega_{0I,j}}, \quad (3) \\ \tan \eta_{\beta,j} &= \frac{B_j^*}{A_j + 2\omega_{0I,j}} \end{aligned}$$

$$U_\eta(H_Z + H_{IS})U_\eta^{-1} = \Delta\omega_{0S}S_z + \sum_j (-\tilde{\omega}_{0I,j}I_{jz} + \tilde{A}_j S_z I_{jz}).$$

We have introduced additional terms to simplify the resulting Hamiltonian, which are given by

$$\begin{aligned} \tilde{\omega}_{0I,j} &= \frac{1}{2}\omega_{0I,j}(\cos \eta_{\alpha,j} + \cos \eta_{\beta,j}) \\ &\quad - \frac{1}{4}A_j(\cos \eta_{\alpha,j} - \cos \eta_{\beta,j}) \\ &\quad - \frac{1}{4}B_j^*(\sin \eta_{\alpha,j} - \sin \eta_{\beta,j}) \quad (4) \\ \tilde{A}_j &= -\omega_{0I,j}(\cos \eta_{\alpha,j} - \cos \eta_{\beta,j}) \\ &\quad + \frac{1}{2}A_j(\cos \eta_{\alpha,j} + \cos \eta_{\beta,j}) \\ &\quad + \frac{1}{2}B_j^*(\sin \eta_{\alpha,j} + \sin \eta_{\beta,j}). \end{aligned}$$

We focus on the effects that the partial diagonalization has on H_M since application of U_χ and U_η to H_{II} is very involved but does not contribute as much insight. Defining $\eta_j = (\eta_{\alpha,j} - \eta_{\beta,j})/2$ for convenience, we obtain

$$\begin{aligned} U_\eta U_\chi H_M U_\chi^{-1} U_\eta^{-1} &= \omega_{1S} \left[S_x \prod_j \cos \eta_j - 2 \sum_j S_y I_{jy} \sin \eta_j \prod_{l \neq j} \cos \eta_l \right. \\ &\quad \left. + 2 \sum_j \sum_{k>j} S_x I_{jy} I_{ky} \sin \eta_j \sin \eta_k \prod_{l \neq j,k} \cos \eta_l - \dots \right] \\ &= \omega_{1S} S(k) \prod_j (\cos \eta_j - i I_{jy} \sin \eta_j), \quad (5) \end{aligned}$$

where the $\sin \eta_j$ are typically small and $\cos \eta_j \approx 1$. The second form of (5) uses $S(k)$; $S(k)$ is evaluated by first expanding the product, then for terms containing an even number of I_{jy} operators, $S(k) = S_x$, and for terms containing an odd number of I_{jy} operators, $S(k) = -iS_y$.⁴⁶

Examining (5), we see that the first term drives off resonant saturation of the electron. The next term drives the usual SE transition, and all other terms drive higher order SE transitions. In this case, the intensities of higher order transitions are a product of several $\sin \eta_j$. Since the η_j , η_k , ... are small, the probability of these transitions becomes rapidly smaller as the number of nuclear spins increases. The matching condition of a specific transition (ignoring H_{II}), for which the electron and nuclear spins j , k , ... are flipped, and nuclear spins p , q , ... are not flipped is given

by

$$\begin{aligned}
 & |S_{\alpha/\beta} I_{j,\alpha/\beta} I_{k,\alpha/\beta} \dots I_{p,\alpha/\beta} I_{q,\alpha/\beta} \dots\rangle \\
 & \rightarrow |S_{\beta/\alpha} I_{j,\beta/\alpha} I_{k,\beta/\alpha} \dots I_{p,\alpha/\beta} I_{q,\alpha/\beta} \dots\rangle \\
 & \pm \Delta\omega_{0S} = (\pm\tilde{\omega}_{0I,j} \pm \tilde{\omega}_{0I,k} \pm \dots) + \frac{1}{2}(\pm\tilde{A}_p \pm \tilde{A}_q \pm \dots),
 \end{aligned}
 \tag{6}$$

where α/β indicates that a spin is in the spin-up or spin-down state, and the sign on a term corresponding to the j th, k th, p th, or q th nucleus depends on its initial state. The matching condition reduces to $\Delta\omega_{0S} = \pm n\omega_{0I}$ when the electron-nuclear coupling of the fixed spins is neglected. However, if there is a strong electron-nuclear coupling to some of the fixed spins, then this coupling cannot be ignored. We do not explicitly calculate $U_\chi U_\eta H_{II} U_\eta^{-1} U_\chi^{-1}$, but note that the nuclear-nuclear couplings in H_{II} , when tilted by U_χ , will lead to an indirect coupling of the electron to the nuclei, and will therefore contribute to the SE mechanism. In our experiments, we observe higher order transitions—transitions involving two or more nuclei—and see that the intensity of these transitions is much higher than predicted by (5). Therefore, the nuclear-nuclear couplings must contribute to the mixing that leads to the DNP enhancement, since the electron-nuclear coupling cannot account for the transition intensity alone.

III. RESULTS AND DISCUSSION

We have performed electron-detected SE-DNP experiments on a 140 GHz pulsed-EPR/DNP system described recently⁴⁰ utilizing a fundamental mode TE₀₁₁ coiled resonator.⁴⁷ In each experiment, the variable frequency electron-electron double resonance (ELDOR) channel of the EPR bridge was used to apply continuous-wave microwave irradiation to the sample. After a period of irradiation and a short delay (10–20 μ s to eliminate any electron coherence), the on-resonance polarization was measured using a Hahn echo, as shown in Figure 1(a). Experiments were performed with samples using 40 mM radical concentration, corresponding to typical concentrations used in DNP experiments.

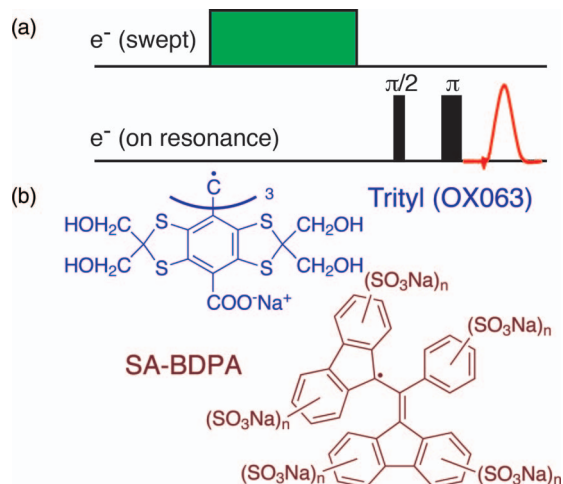


FIG. 1. (a) Pulse sequence for the electron-detected SE. (b) Structures of trityl (OX063) and SA-BDPA radicals used for SE experiments.

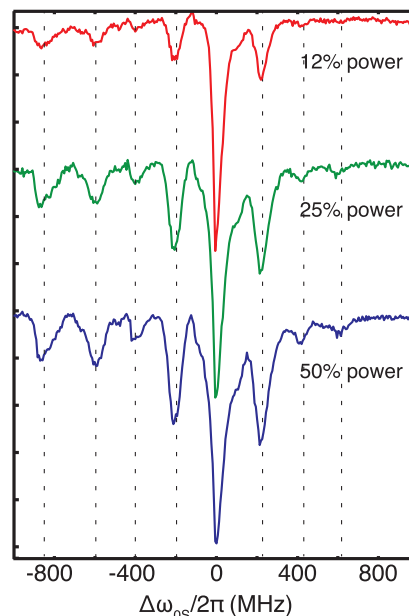


FIG. 2. Frequency sweep of the electron-detected solid effect of 40 mM trityl in 60:25:15 (v/v/v) ¹³C-glycerol:D₂O:H₂O at 80 K. The power dependence of SE is shown for 5 ms of microwave irradiation. Electron polarization was measured near the center of the trityl EPR spectrum (4993.6 mT). Microwave field strengths are given in the figure below each frequency sweep, and have been determined for $\Delta\omega_{0S} = 0$.

Figure 2 shows the results of irradiating the sample at various frequencies, using three different microwave field strengths ($\gamma B_1 = 2.5, 1.7, 1.2$ MHz). As expected, the electron polarization is depleted when irradiating on resonance with the EPR spectrum, and when the microwave frequency is offset by ± 212 MHz, corresponding to the SE condition ($\Delta\omega_{0S} = \pm\omega_{0I}$). However, polarization depletion is also observed at $\Delta\omega_{0S} = \pm n\omega_{0I}$, where $n = 2, 3, 4$. Unfortunately, the high quality factor (Q) of the cavity, which allows for efficient solid effect also leads to a narrow frequency bandwidth of the cavity—hence attenuation of some of the transitions on the high-frequency side of the spectrum.

Observation of transitions for $n > 1$ is not entirely unexpected: Higher order terms in (5) suggest that higher order transitions should exist. Also, the $n = 2$ transition was observed via ¹H NMR by de Boer, although the relative intensity was far lower than observed here.^{48,49} In fact, the intensities observed here are far higher than one should expect. The strongest e-¹H dipole coupling is not expected to be more than several MHz,⁵⁰ so even the $n = 2$ intensity should be at most a few percent of the $n = 1$ intensity, based on (5). One should note, though, that (5) does not take account of the contribution of nuclear-nuclear couplings. Therefore, strong nuclear mixing contributes to the observation of intense, higher order contributions. Also, note that the relative intensities of the various SE transitions remain similar in the three experiments in Figure 2. This is consistent with (5), where all SE transition amplitudes are linear to the microwave field strength (ω_{1S}). One expects the degree of electron saturation for the SE to be proportional to the square of the transition amplitude when the relaxation rate constant is significantly larger than the transition amplitude, and the electron does not become fully

saturated. One can see in Figure 2 that the electron is not fully saturated. Because the electron $T_2 \approx 1 \mu\text{s}$,⁴⁶ the decay rate of the electron coherence is on the order of the microwave field strength (several MHz). However, for $n = 1-4$ transitions, the decay rate is much larger than the transition amplitude, due to scaling of these transitions by the nuclear Larmor frequency. We see then that the presence of higher order SE transitions is not a result of higher order dependence on the microwave field strength, but results from a strong network of electron-nuclear and nuclear-nuclear couplings. We further note that the observation of higher order transitions for $n = 2, 3, 4$ indicates that it is possible that similar high order transitions contribute to DNP at the usual, $n = 1$, condition. For example, if three nuclei and one electron begin in the state $|S_{\alpha}I_{j,\alpha}I_{k,\alpha}I_{l,\beta}\rangle$, then all spins can be inverted, yielding the final state $|S_{\beta}I_{j,\beta}I_{k,\beta}I_{l,\alpha}\rangle$, and having a transition frequency of $\Delta\omega_S \approx \omega_{0,l}$, according to (6). Thus, this would be observed at the $n = 1$ condition, although the transition itself involves three nuclear spins. We believe this type of mechanism can play a major role in polarizing nuclei that are strongly coupled to the electron.

In Figure 3, we show similar experimental results, using a slightly different sample and different microwave tuning conditions. In this case, we vary the duration of the microwave irradiation and are able to observe the equilibration of the electron polarization during the SE. As one might expect, electron polarization is destroyed almost immediately when applying a microwave field on-resonance with the EPR spectrum. However, when the microwave frequency is set to a SE condition, one can see the polarization is depleted more slowly since in

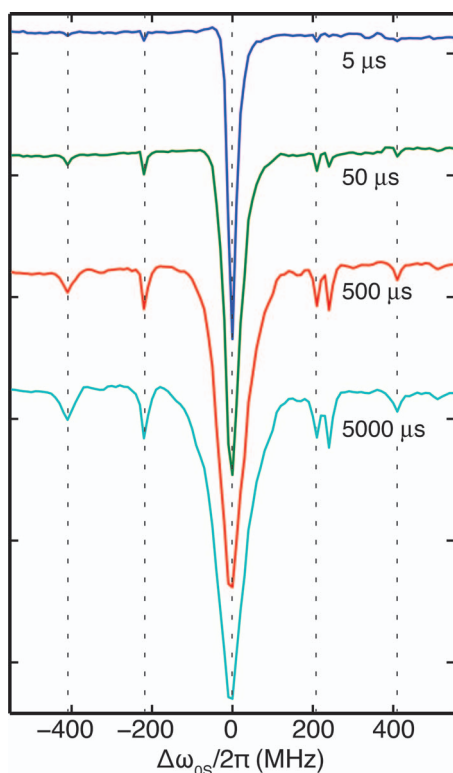


FIG. 3. Frequency sweep of the electron-detected SE of 40 mM trityl in 60:25:15 (v/v/v) ^{13}C -glycerol: D_2O : H_2O at 80 K. The duration of the microwave irradiation was varied for the four sweeps. The microwave field strength was ~ 2.5 MHz at $\Delta\omega_{0S} = 0$.

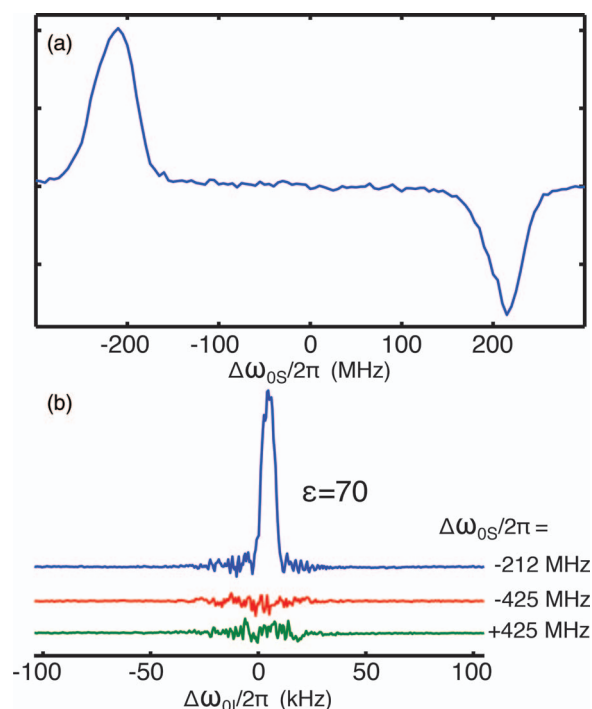


FIG. 4. (a) SE-DNP frequency profile observed after 10 s microwave irradiation via NMR cross polarization from ^1H to ^{13}C . (b) NMR spectra at the SE-DNP conditions $\Delta\omega_{0S} = -\omega_{0I}$ and $\Delta\omega_{0S} = \pm 2\omega_{0I}$, also observed via CP, where no significant enhancement can be seen for $\Delta\omega_{0S} = \pm 2\omega_{0I}$. The microwave field strength is ~ 2.5 MHz.

this case the transition moments are much smaller as given in (5). The additional peak at $\Delta\omega_{0S} = +240$ MHz is an artifact of the EPR system. It is not saturation due to SE, as can be seen by the different rate of buildup from the peak at $\Delta\omega_{0S} = +210$ MHz.

One may note that we have used ^{13}C labeled glycerol in our experiments. This was done so that one could observe nuclear polarization via a ^1H - ^{13}C cross polarization experiment, as shown in Figure 4. Direct observation of ^1H polarization can be difficult due to a large ^1H background, whereas ^{13}C does not suffer from background signal. It might be expected to see peaks in Figures 2 and 3 resulting from polarization transfer to ^{13}C . However, one should note that coupling to ^{13}C is smaller than to ^1H , both due to the smaller ^{13}C gyromagnetic ratio, and also because some ^1H are part of the radical molecule, whereas the radical is not ^{13}C labeled, so that most ^{13}C nuclei will be further away. Furthermore, peaks arising from couplings to ^{13}C for the $n = 1$ condition will be overlapping the peak resulting from direct saturation of the radical.

In Figure 4(a), we show a frequency profile for which we observe the ^1H polarization resulting from SE, rather than observing the electron polarization. An NMR cross polarization experiment was used to transfer ^1H polarization to ^{13}C , after 10 s of microwave irradiation. As expected, we see DNP enhancements at the usual SE matching condition, $\Delta\omega_{0S} = \pm\omega_{0I}$. In light of our electron-detected SE results, one might expect to also see enhancements at $\Delta\omega_{0S} = \pm n\omega_{0I}$ (for $n = 2, 3, 4$). However, this was not the case. In Figure 4(b), the microwave frequency was set to meet the condition $\Delta\omega_{0S} = \pm 2\omega_{0I}$ and also the microwave cavity was returned to

obtain maximum microwave field strength. Whereas at the $n = -1$ condition, one sees an enhancement of 70, no significant enhancement is observed at the $n = \pm 2$ conditions.

The absence of bulk nuclear enhancement at the $n = \pm 2$ SE conditions, despite a significant polarization loss observed on the electron, is consistent with our recent model of electron to bulk polarization transfer.³⁸ In our model, we proposed that electron polarization was transferred directly to both nearby and bulk nuclei. However, the polarization transfer to nearby nuclei is not subsequently transferred via spin-diffusion to the bulk, but rather fast nuclear spin-lattice relaxation near the electron destroys this polarization. As a result, the nearby nuclei deplete the amount of polarization available for direct electron-nuclear transfer to the bulk nuclei. The results shown here for the $n = \pm 2$ SE condition suggest that polarization loss observed on the electron is primarily a result of transfer of polarization to nearby nuclei, since the η_j are largest for these nuclei, making the transfer more likely. However, because these nuclei do not efficiently transfer polarization to the bulk, a large loss of polarization is observed on the electron without a significant gain of bulk nuclear polarization. One also should note that direct observation of polarization on these nearby nuclei is difficult, because of their proximity to the electron that can result in very broad linewidths, and that there are only a few nuclei that are considered nearby to the electron, whereas there are many nuclei in the bulk. Therefore, without transfer of polarization between nuclei near the electron and the bulk nuclei, we would not expect to observe an NMR signal, even if nuclei near the electron are highly polarized.

In Figure 5, we illustrate the electron-detected SE experiment for the SA-BDPA radical, with a 10 μ s irradiation time. For this frequency sweep, we see the transitions for $n = 1, 2$. In contrast to trityl, we see a large number of individual peaks around each transition. In contrast to trityl, for which there are very few protons near the radical center, the SA-BDPA molecule has 14–17 protons with large hyperfine couplings.⁷ Hovav *et al.* predict the splitting of the DNP matching condition due to the electron-nuclear couplings of nearby nuclei,³⁶ as do we in (6). When comparing the trityl and SA-BDPA fre-

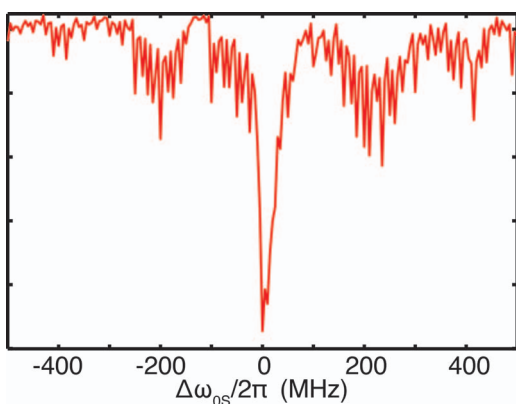


FIG. 5. Frequency sweep of the electron-detected solid effect of 40 mM SA-BDPA in 60:40 (v/v) ^{13}C -glycerol: D_2O at 80 K. Microwave irradiation is applied for 10 μ s, followed by polarization detection at the center of the SA-BDPA spectrum (4995.05 mT). The microwave field strength was ~ 2.5 MHz at $\Delta\omega_{0S} = 0$.

quency sweeps, we see that this effect is clearly demonstrated here. Also, we note that one would not normally be able to resolve this splitting when observing SE via NMR detection; the many different orientations of the radical, each with a slightly different Larmor frequency, will broaden the condition and cover the splitting. However, due to the orientation-selective nature of the Hahn echo in high field EPR, we are able to observe the splitting.

IV. CONCLUSIONS

We have shown via electron-detected SE experiments that it is possible to observe depletion of polarization of the electron spin via the SE mechanism. This occurs both for the expected $n = 1$ transition, but also for $n = 2, 3, 4$. Observation of these higher order transitions is thought to be a result of both strong electron-nuclear and nuclear-nuclear couplings. Despite the fact that electron saturation occurs for the $n = \pm 2$ condition, bulk nuclear polarization is not observed at this condition. This is consistent with the polarization of nuclei that are nearby to the electron. We predicted, in our recent model of the solid effect, that nuclei near the electron do not transmit polarization to the bulk. The current result, therefore, adds further supporting evidence for this model of polarization transfer, and suggests that complex, higher order transitions may further accelerate the transfer of polarization to these nearby nuclei, but not to bulk nuclei. The result also suggests that it should be possible to improve SE DNP conditions via local reduction of ^1H polarization near the electron, while maintaining higher concentration throughout the sample.

ACKNOWLEDGMENTS

This research was supported by the National Institutes of Health through Grant Nos. EB002804 and EB002026 to R.G.G. and Grant No. GM095843 to T.M.S. B.C. acknowledges a fellowship from the Deutsche Forschungsgemeinschaft (Research Fellowship CO 802/1-1).

¹T. R. Carver and C. P. Slichter, *Phys. Rev.* **92**(1), 212 (1953).

²A. W. Overhauser, *Phys. Rev.* **92**(2), 411 (1953).

³C. Song, K.-N. Hu, C.-G. Joo, T. M. Swager, and R. G. Griffin, *J. Am. Chem. Soc.* **128**(35), 11385 (2006).

⁴Y. Matsuki, T. Maly, O. Ouari, H. Karoui, F. Le Moigne, E. Rizzato, S. Lyubenova, J. Herzfeld, T. F. Prisner, P. Tordo, and R. G. Griffin, *Angew. Chem.* **48**(27), 4996 (2009).

⁵E. L. Dane, B. Corzilius, E. Rizzato, P. Stocker, T. Maly, A. A. Smith, R. G. Griffin, O. Ouari, P. Tordo, and T. M. Swager, *J. Org. Chem.* **77**(4), 1789 (2012).

⁶M. K. Kieseewetter, B. Corzilius, A. A. Smith, R. G. Griffin, and T. M. Swager, *J. Am. Chem. Soc.* **134**, 4537–4540 (2012).

⁷O. Haze, B. Corzilius, A. A. Smith, R. G. Griffin, and T. M. Swager, *J. Am. Chem. Soc.* **134**(35), 14287 (2012).

⁸S. Macholl, H. Johannesson, and J.-H. Ardenkjaer-Larsen, *Phys. Chem. Chem. Phys.* **12**(22), 5804 (2010).

⁹B. Corzilius, A. A. Smith, A. B. Barnes, C. Luchinat, I. Bertini, and R. G. Griffin, *J. Am. Chem. Soc.* **133**(15), 5648 (2011).

¹⁰A. Zagdoun, G. Casano, O. Ouari, G. Lapadula, A. J. Rossini, M. Lelli, M. Baffert, D. Gajan, L. Veyre, W. E. Maas, M. M. Rosay, R. T. Weber, C. Thieuleux, C. Coperet, A. Lesage, P. Tordo, and L. Emsley, *J. Am. Chem. Soc.* **134**(4), 2284 (2012).

¹¹K. Hu, H. Yu, T. Swager, and R. Griffin, *J. Am. Chem. Soc.* **126**(35), 10844 (2004).

- ¹²V. S. Bajaj, M. K. Hornstein, K. E. Kreisler, J. R. Sirigiri, P. P. Woskov, M. L. Mak-Jurkauskas, J. Herzfeld, R. J. Temkin, and R. G. Griffin, *J. Magn. Reson.* **189**(2), 251 (2007).
- ¹³A. B. Barnes, M. L. Mak-Jurkauskas, Y. Matsuki, V. S. Bajaj, P. C. A. van der Wel, R. DeRocher, J. Bryant, J. R. Sirigiri, R. J. Temkin, J. Lugtenburg, J. Herzfeld, and R. G. Griffin, *J. Magn. Reson.* **198**(2), 261 (2009).
- ¹⁴A. C. Torrezan, S.-T. Han, I. Mastovsky, M. A. Shapiro, J. R. Sirigiri, R. J. Temkin, A. B. Barnes, and R. G. Griffin, *IEEE Trans. Plasma Sci.* **38**, 1150–1159 (2010).
- ¹⁵J. Leggett, R. Hunter, J. Granwehr, R. Panek, A. J. Perez-Linde, A. J. Horsewill, J. McMaster, G. Smith, and W. Kockenberger, *Phys. Chem. Chem. Phys.* **12**(22), 5883 (2010).
- ¹⁶S. Jannin, A. Bernet, S. Colombo, and G. Bodenhausen, *Chem. Phys. Lett.* **517**(4–6), 234 (2011).
- ¹⁷V. S. Bajaj, M. L. Mak-Jurkauskas, M. Belenky, J. Herzfeld, and R. G. Griffin, *Proc. Natl. Acad. Sci. U.S.A.* **106**(23), 9244 (2009).
- ¹⁸M. Rosay, J. Lansing, K. Haddad, W. Bachovchin, J. Herzfeld, R. Temkin, and R. Griffin, *J. Am. Chem. Soc.* **125**(45), 13626 (2003).
- ¹⁹M. L. Mak-Jurkauskas, V. S. Bajaj, M. K. Hornstein, M. Belenky, R. G. Griffin, and J. Herzfeld, *Proc. Natl. Acad. Sci. U.S.A.* **105**(3), 883 (2008).
- ²⁰G. T. Debelouchina, M. J. Bayro, P. C. A. van der Wel, M. A. Caporini, A. B. Barnes, M. Rosay, W. E. Maas, and R. G. Griffin, *Phys. Chem. Chem. Phys.* **12**(22), 5911 (2010).
- ²¹Ü. Akbey, W. T. Franks, A. Linden, S. Lange, R. G. Griffin, B.-J. van Rossum, and H. Oschkinat, *Angew. Chem., Int. Ed.* **49**(42), 7803 (2010).
- ²²M. J. Bayro, G. T. Debelouchina, M. T. Eddy, N. R. Birkett, C. E. MacPhee, M. Rosay, W. E. Maas, C. M. Dobson, and R. G. Griffin, *J. Am. Chem. Soc.* **133**(35), 13967 (2011).
- ²³A. Lesage, M. Lelli, D. Gajan, M. A. Caporini, V. Vitzthum, P. Mieville, J. Alauzun, A. Roussey, C. Thieuleux, A. Mehdi, G. Bodenhausen, C. Coperet, and L. Emsley, *J. Am. Chem. Soc.* **132**(44), 15459 (2010).
- ²⁴B. D. Armstrong and S. Han, *J. Am. Chem. Soc.* **131**(31), 4641 (2009).
- ²⁵H. Zeng, Y. Lee, and C. Hilty, *Anal. Chem.* **82**, 8897 (2010).
- ²⁶C. D. Jeffries, *Phys. Rev.* **117**(4), 1056 (1960).
- ²⁷C. D. Jeffries, *Phys. Rev.* **106**(1), 164 (1957).
- ²⁸A. V. Kessenikh, V. I. Lushchikov, A. A. Manenkov, and Yu. V. Taran, *Sov. Phys. Solid State* **5**(2), 321 (1963).
- ²⁹A. V. Kessenikh, A. A. Manenkov, and G. I. Pyatnitskii, *Sov. Phys. Solid State* **6**(3), 641 (1964).
- ³⁰D. S. Wollan, *Phys. Rev. B* **13**, 3671 (1976).
- ³¹M. Goldman, *Spin Temperature and Nuclear Magnetic Resonance in Solids* (Clarendon Press, Oxford, 1970).
- ³²M. J. Duijvestijn, R. A. Wind, and J. Smidt, *Physica B & C* **138**(1–2), 147 (1986).
- ³³R. A. Wind, M. J. Duijvestijn, C. van der Lugt, A. Manenschijn, and J. Vriend, *Prog. Nucl. Magn. Reson. Spectrosc.* **17**, 33 (1985).
- ³⁴G. Jeschke and A. Schweiger, *Mol. Phys.* **88**(2), 355 (1996).
- ³⁵K.-N. Hu, G. T. Debelouchina, A. A. Smith, and R. G. Griffin, *J. Chem. Phys.* **134**(12), 125105 (2011).
- ³⁶Y. Hovav, A. Feintuch, and S. Vega, *J. Magn. Reson.* **207**(2), 176 (2010).
- ³⁷Y. Hovav, A. Feintuch, and S. Vega, *J. Chem. Phys.* **134**(7), 074509 (2011).
- ³⁸A. A. Smith, B. Corzilius, A. B. Barnes, T. Maly, and R. G. Griffin, *J. Chem. Phys.* **136**(1), 015101 (2012).
- ³⁹B. Corzilius, A. A. Smith, and R. G. Griffin, *J. Chem. Phys.* **137**(5), 054201 (2012).
- ⁴⁰A. A. Smith, B. Corzilius, J. Bryant, R. DeRocher, P. P. Woskov, R. J. Temkin, and R. G. Griffin, *J. Magn. Reson.* **223**, 170 (2012).
- ⁴¹P. Schosseler, T. Wacker, and A. Schweiger, *Chem. Phys. Lett.* **224**(3–4), 319 (1994).
- ⁴²E. R. Davies, *Phys. Lett. A* **47**(1), 1 (1974).
- ⁴³W. B. Mims, *Proc. R. Soc. London, Ser. A.* **283**, 452 (1965).
- ⁴⁴L. Rapatskiy, N. Cox, A. Savitsky, W. M. Ames, J. Sander, M. M. Nowaczyk, M. Rögner, A. Boussac, F. Neese, J. Messinger, and W. Lubitz, *J. Am. Chem. Soc.* **134**, 16619 (2012).
- ⁴⁵V. Nagarajan, Y. Hovav, A. Feintuch, S. Vega, and D. Goldfarb, *J. Chem. Phys.* **132**(21), 214504 (2010).
- ⁴⁶G. Jeschke and A. Schweiger, *J. Chem. Phys.* **105**(6), 2199 (1996).
- ⁴⁷V. Weis, M. Bennati, M. Rosay, J. A. Bryant, and R. G. Griffin, *J. Magn. Reson.* **140**(1), 293 (1999).
- ⁴⁸W. de Boer, *J. Low Temp. Phys.* **22**(1–2), 185 (1976).
- ⁴⁹A. Abragam and M. Goldman, *Rep. Prog. Phys.* **41**(3), 395 (1978).
- ⁵⁰M. Bowman, C. Mailer, and H. Halpern, *J. Magn. Reson.* **172**(2), 254 (2005).